AN INTERFEROMETRIC STUDY OF HEAT TRANSFER IN TURBULENT JET FLOWS

V. I. Vishnyakov, A. M. Makarov, L. K. Martinson, and K. B. Pavlov

Inzhenerno-Fizicheskii Zhurnal, Vol. 15, No. 2, pp. 193–202, 1968

UDC 532.517.4

An experimental investigation is undertaken of the distribution of temperature and heat transfer in plane turbulent flows, involving the use of the Zender-Mach interferometer.

The extensive literature data on jet flows pertain, for the most part, to the aerodynamics of flow [1–5]. However, the calculation of heat transfer in jet flows is possible only if we know the temperature distribution within the jet. The interferometry method has gained widespread acceptance in recent times in the study of heat-transfer processes [6–10]. This method of determining the temperature fields in transparent media is based on the relationship between the refractive index of materials and temperature, and it exhibits a significant advantage over the probe methods, since it makes it possible to determine the temperature distribution simultaneously over the entire area of observation, without introducing any disruptions of the aerodynamics and temperature field of the process being investigated [11–13]. The inertia of such a temperature sensor, i.e., the time between two successive temperature measurements at a given point in the field, is thus virtually determined by the speed of photography. The interferometry method makes it possible to obtain information on temperature distribution for a number of cases of turbulent jet flows of practical interest, some of which will be dealt with in this paper.

THE EXPERIMENTAL SET-UP

For the purposes of the investigation we developed an installation which provides for a regulated supply of heated gas into a nozzle. The air from a rotational supercharger is supplied into a static-pressure chamber and is then transmitted through a VT-40/400 heater through thermally insulated tubing to the nozzle.

We used plane-slotted shaped nozzles exhibiting outlet cross sections of 1×100, 2×50, and 1×50 mm and a constriction ratio of 20:1, with these nozzles made of brass. The air was supplied to the nozzle by means of a conical adapter tube. Immediately ahead of the inlet to the shaped channel of the nozzle we installed a grid with small cells. This permitted us to equalize the velocity of the airstream over the entire length of the slot and to achieve uniform discharge. To reduce the convection currents from the nozzle casing, provision was made for the thermal shielding of the casing by means of two thermal-insulation layers made of asbestos, between which thin copper tubing was coiled. The cooling water was continuously circulated through the tubing, so that the upper thermal-insulation layer exhibited a temperature equal to that of the ambient air. Thus it became possible to eliminate distortions of the interference pattern introduced by convection.

The temperature of the air being discharged from the nozzle was regulated by a T8S1 semiconductor temperature sensor mounted inside the nozzle. The air flow rate through the nozzle was varied by means of control valves and it was determined by a DR-11 induction flow-rate sensor which covered a measurement range from 0.9 to 2.5 l/sec. The visualization of the flow was achieved with an IZK-454 interferometer employing the Zender-Mach system [14], in which the diameter of the observed field was about 220 mm.

The nozzles were located in one of the arms of the interferometer so that the light beams were directed parallel to the nozzle slot. The interference bands of equal thickness, localized in the plane of the nozzles, were focused onto photographic film. Visual observations were thus simultaneously achieved.

THE EXPERIMENTAL METHOD

The interferometry method of determining the temperature fields is based on the following physical phenomenon. If there is a change in the refraction index along the path of the light beams traveling in one of the arms of the interferometer, there is a shift in the interference pattern, and measurement of this shift enables us to determine the change in the refractive index.

In this experiment the change in the refractive index of the air was due exclusively to the change in temperature, since in the flows under consideration, in most cases, pressure was constant [15].

As is well known [16], the expression for the determination of the temperature T(y) at any point on the interference band can be written in terms of the temperature T_0 of the unperturbed gas in the form

$$T(y) = \frac{T_0}{1 - \dfrac{\delta_\lambda(y)}{L(n_0 - 1)}}, \qquad (1)$$

where L is the length of the light beam in the perturbed region (in the case under consideration it is the thickness of the jet measured parallel to the slot of the nozzle), $\delta_\lambda(y)$ is the shift in the interference band, and n_0 is the refractive index in the unperturbed region.

Thus, interpretation of the interference pattern reduces virtually to the determination of the shift $\delta_\lambda(y)$. The determination of the length L presents some difficulty. In first approximation, it may be assumed

equal to the nozzle-slot length L_0. However, to increase the accuracy of determining temperature, the quantity L was found with consideration of the jet flare angle by the two-wavelength method discussed below. For this purpose, interference filters with a narrow passband were mounted in two separate receiver portions of the interferometer. The filter in one of the receiver portions exhibited a key-in region near $\lambda_1 = 5900$ Å, and near $\lambda_2 = 4480$ Å in the other.

Let us consider the case of a free stream being discharged from a plane-slot nozzle with a slot length L_0. The discharging jet represents the perturbed region along the path of the light rays. The length of this region for the rays of light passing the nozzle outlet (x = 0) is equal to the nozzle-slot length L_0, while for the rays passing at a distance $x > 0$ it is, correspondingly, $L = L_0 + \Delta L$.

According to [17], the magnitude of the shift in the interference bands, expressed in terms of wavelength, for the jet cross section is written as follows:

$$x = 0 \begin{cases} \delta_{\lambda_1} = L_0 (n_{0_1} - n_1), \\ \delta_{\lambda_2} = L_0 (n_{0_2} - n_2), \end{cases} \tag{2}$$

$$x > 0 \begin{cases} \delta'_{\lambda_1} = L (n_{0_1} - n'_1), \\ \delta'_{\lambda_2} = L (n_{0_2} - n'_2). \end{cases} \tag{3}$$

Subscripts 1 and 2 denote the quantities pertaining to the corresponding wavelengths, while the prime denotes the quantities for the cross sections at a distance $x > 0$.

Using the Gladstone-Dale formula [17], from (2) and (3) we have

$$L = L_0 \frac{\delta'_{\lambda_1} (n_{0_2} - 1) - \delta'_{\lambda_2} (n_{0_1} - 1)}{\delta_{\lambda_1} (n_{0_2} - 1) - \delta_{\lambda_2} (n_{0_1} - 1)} . \tag{4}$$

Thus, the method of two wavelengths presented above makes it possible simultaneously to find both the dimensions of the region in the direction of the light rays, as well as the temperature distribution in this region. If we bear in mind that the quantity L is associated with the jet flare angle α by the relationship

$$L = L_0 + 2x \operatorname{tg} \frac{\alpha}{2} , \tag{5}$$

it is sufficient to find the length L only in some single cross section of the jet.

The calculations for the free and semibounded jets were carried out on the basis of formulas (4) and (5). Thus, for the free jet the flare angle in the direction of the light beams was 3–5°. The found values of the angle for the semibounded jet were 6–8°. Thus we see that the change in the thickness of the jet in the direction of the light rays is slight; however, it may be substantial at greater distances from the nozzle outlet. Corresponding correction factors were taken into consideration in the calculations of the temperature fields.

From the well-known temperature distribution we can determine the coefficient of heat transfer from the jet to the heat-transfer plate. The local heat flow was determined directly from the interferograms.

The local heat-transfer coefficient Nu(x) is determined from the relationship

$$\mathrm{Nu}(x) = \frac{x}{T_e - T_w} \left(\frac{\partial T}{\partial y} \right)_{y=0} . \tag{6}$$

Differentiating (1) with respect to y and substituting into (6), we have

$$\mathrm{Nu}(x) = \frac{x}{T_e - T_w} \times \frac{T_0}{[L (n_0 - 1)] \left[1 - \dfrac{\delta_\lambda (0)}{L (n_0 - 1)} \right]^2} \left(\frac{\partial \delta_\lambda}{\partial y} \right)_{y=0} . \tag{7}$$

The quantity $(\partial \delta_\lambda / \partial y)_{y=0}$ can be found graphically from the interferograms from the inclination of the interference bands with consideration of band width.

ANALYSIS OF RESULTS

On the basis of the method considered above, we carried out the following series of experiments: a) a freely submerged turbulent jet; b) interacting jets; c) semibounded jets. The first series of experiments served simultaneously as the preliminary refinement and testing of the method used. The second and third series were valid from the practical standpoint.

For example, we find jets (from nozzles) impinging on each other at some angle in spraying equipment, ventilation engineering, and in pulsating MHD generators. The use of semibounded jets finds application for industrial cooling or heating, because of the excellent accuracy of regulation which these jets permit.

a) The freely submerged turbulent jet. We investigated free heated submerged turbulent jets of air being discharged from a plane nozzle with slot dimensions of 1 × 50 mm and 2 × 50 mm. For greater reliability and control of results reproducibility, all of the tests were carried out for the identical initial velocity (on the order of 20 m/sec).

For the change in the maximum excess temperature along the jet axis we found excellent agreement between the experimental data and those theoretically calculated on the basis of the formula presented in Abramovich's book [18] for a plane, turbulent, slightly heated ($T_S/T_0 < 1.1$) jet:

$$\frac{\Delta T_m}{\Delta T} = \frac{1.04}{\sqrt{T_s/T_0}\sqrt{2ax/b}} , \tag{8}$$

where $\Delta T_m = T_m - T_0$ is the difference between the temperatures at the jet axis and in the surrounding space, $\Delta T = T_S - T_0$ is the difference between the temperatures at the nozzle outlet and in the surrounding space, x is the distance from the given cross section to the initial section, b is the width of the initial cross section of the jet, and a is the coefficient of the plane-jet structure.

It should be noted that the best agreement is found when a is equal to 0.12. As shown by the experiment, it is also possible to use (8) to calculate the profiles of the maximum excess temperature for jets in which $T_S/T_0 > 1.1$. Formula (8) was used to carry out the calculations for jets in which $T_S/T_0 = 2$. No significant deviations from the experimental data were noted.

We found that the jet flare angle increases as the temperature of the discharging air rises and with a reduction in the flow rate. However, this increase is comparatively small and does not exceed 3° in the

temperature range from 303 to 573° K when the flow rate is constant. We note that the width of the nozzle slot has absolutely no effect on the jet flare angle.

b) The interaction of two jets. On interaction of two jets, as a result of the mixing of these jets, a single, rather complex resulting gas stream is formed. Until recently, very little attention has been devoted to the quantitative relationships governing the mixing of jets, even in the very simplest of cases in the theory of jets (for example, for isothermal gas jets at normal pressure). Some results from a study on the mixing of two plane free turbulent air jets are presented in this section, since the characteristic features involved in the mixing process appear most clearly in the case of plane jets. The air jets pass into the atmosphere from nozzles exhibiting outlet cross sections of 1 × 50 mm.

The discharge velocity was 20 m/sec. One of the nozzles could be mounted with respect to the other at various angles from zero to 90°, with the distance between the nozzle outlet sections set at 40 mm.

A number of experiments were carried out for jet interaction at angles of 30, 60, and 90°. The difference between the discharge temperatures was 30° C. Figure 1 shows a typical isotherm pattern for the case at which the jets are interacting at an angle of 60°. These results indicate that the axes of the two jets, in the process of interaction, deviate from the initial direction. The deformation of the axes is considered in the examination of the temperature fields. The temperature maxima in these jets converge with increasing distance from the nozzle outlets, and then diverge markedly, forming a single resulting flow which apparently consists of two deformed jets between which there exists a weakly heated region.

It is interesting to note that the flare angle of the resulting flow, given an identical flow rate for the air through both of the nozzles, is approximately equal to the angle of incidence. Thus, the reflection angle is equal to the angle of incidence and is virtually independent of the difference between the initial temperatures at which the jets are discharged.

c) Semibounded plane turbulent jets. The motion of a gaseous medium in a semibounded jet is complex. Various forms of the boundary layer—the wall layer (laminar and turbulent)—are combined here with the free-jet boundary layer. The complex structure of the boundary layer governs the difficulty in predicting the

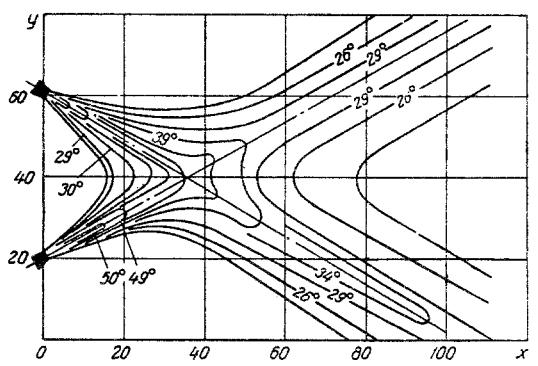

Fig. 1. Chart of isotherms for two interacting jets (x, y, mm).

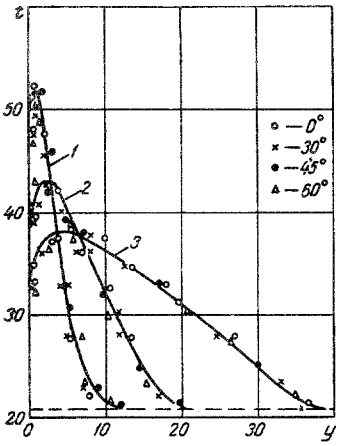

Fig. 2. Temperature (° C) profiles at various sections (mm) of semi-infinite jet for angles of attack φ = 0, 30, 45, and 60°: 1) x/b = 68; 2) 146; 3) 300.

fundamental quantitative relationships governing the propagation of the jet and the development of methods for its calculation. Particular attention was devoted in the study of the semibounded jet to the problem of the temperature distribution and the question of heat transfer. The heated jets of air flowing from the nozzle impinged on the heat-transfer plate. The rotation mechanism for the heat-transfer plate made it possible to alter the angle of jet incidence from 0 to 90°. The vertical-displacement mechanism for the plate also made it possible to deal with those cases in which the outlet cross sections of the nozzle were separated from the plate at distances varying from 0 to 100 mm. The velocity of the air jet at the initial cross section was 25 m/sec.

The heat-transfer plate was made of brass (3 mm thick), whose inside surface was cooled with water to ensure the steadiness of the process. In all of the experiments the outside surface of the plate was kept at a temperature of 17° C.

Figure 2 shows the profiles of the temperatures which changed at various cross sections of the jet when the discharge temperature was T_S = 363° C.

The generalized relationships for the distribution of the excess temperature across the jet for various cross sections and angles of attack are shown in Fig. 3 in the coordinates $\Delta T_y/\Delta T_e = f(x/b)$, where $\Delta T_y = T_y - T_0$ is the difference between the temperatures at the given point of the jet and in the surrounding relatively cold air, and $\Delta T_e = T_e - T_0$ is the difference between the temperatures at the wall surface and the ambient medium. As we can see from this figure, the universality of the temperature profiles for the various cross sections indicate the self-similarity of the flow. Processing of the experimental data permits us to propose the following formulas for the distribution of the temperatures in the transverse cross sections of the jet:

the wall temperature boundary layer $0 < y < \delta_T$

$$\frac{T_m - T_y}{T_m - T_e} = \left[1 - \left(\frac{y}{\delta_T}\right)^{0.23}\right], \qquad (9)$$

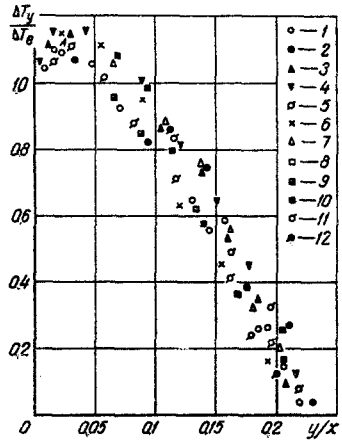

Fig. 3. Universal temperature profile of turbulent semi-infinite jets at initial outflow temperature T_S = 353° K. Values of x/b when angle of attack φ = 0°: 1) 34; 2) 73; 3) 110; 4) 150; φ = 30°: 5) 34; 6) 62; 7) 100; 8) 120; φ = 60°: 9) 34; 10) 73; 11) 110; 12) 150.

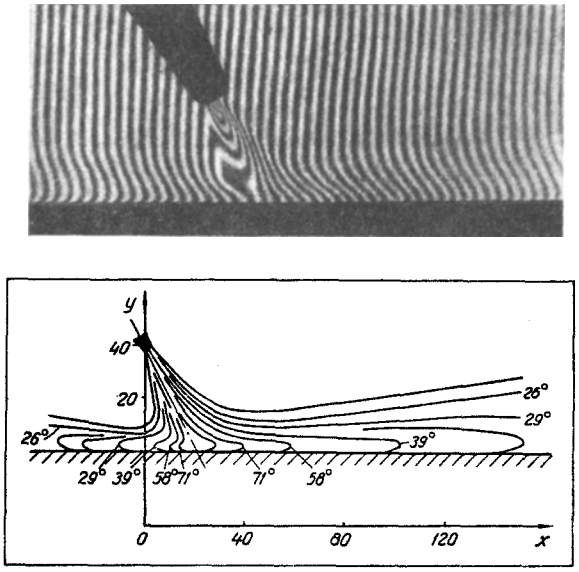

Fig. 4. Interferogram and chart of isotherms of turbulent semi-infinite jet when nozzle outlet is at a distance of 40 mm from the heat-transfer plane of the plate for an angle of attack φ = 62° (T_S = 371° K).

the jet boundary layer $\delta_T \leq y \leq \delta_T + b_T$

$$\frac{T_y - T_0}{T_m - T_0} = \left[1 - \left(\frac{y - \delta_T}{b_T}\right)^{1.3}\right]^2. \qquad (10)$$

It should be pointed out that the exponent in (9) for (y/δ_T) is a function of the heat-transfer conditions. Thus, for example, on interaction of a heated turbulent jet with a marble plate, the exponent is not equal to 0.23, but to 0.35–0.5. This applies equally to (10).

It has been established that when the nozzle outlet touches the surface of the plate, regardless of the angle with which the jet impinges on the plate, the angle of jet flare remains approximately constant. This angle changes little over a wide range of temperatures.

The thicknessess of the temperature (δ_T) and of the jet (b_T) boundary layers can be expressed in terms of the over-all jet thickness by the following relationships:

$$\delta_T = 0.11B_x, \quad b_T = 0.89B_x. \qquad (11)$$

The over-all thickness of the jet is proportional to the distance x from the nozzle outlet and is given by

$$B_x = 0.243x. \qquad (12)$$

Comparing the semibounded jet with the free jet, we can draw the following conclusions.

1. The flare angle of the semibounded jet is smaller by a factor of approximately two than in the case of a free jet, given an identical discharge regime. Thus, for example, at a discharge temperature of 80° C, the former amounts approximately to 13°, while the latter amounts to 25°.

2. The relationships governing the changes in maximum temperature along the jet for semibounded and free jets are similar.

Below we present the experimental results for the case in which the outlet cross section of the nozzle was at a distance of 40 mm from the plane of the heat-transfer plate. Figure 4 shows the interferogram and isotherm pattern for the case in which the nozzle axis makes an angle of 62° with the plane of the plate. This figure can be used to render judgment as to the turning radius of the jet and the flare angle.

The flare angle for the jet impinging perpendicularly on the plane of the plate amounts to (7 – 9) $\pi/180$ rad, while the over-all thickness of the boundary layer is given by B_X = 0.122 x, where x is the distance from the intersection of the upper jet boundary with the plane of the plate. For jets impinging on the plane of the plate at an angle of 30°, B_X = 0.118x, while at an angle of 60°, B_X = 0.12x in the direction of the obtuse angle and B_X = 0.15x in the direction of the acute angle (we refer to the angles formed by the axis of the jet and the plane of the plate). The thickness of the wall temperature layer for these jets can be expressed by the general relationship

$$\delta_T = 0.12B_x. \qquad (13)$$

Table 1 gives the values of the temperatures for the cross section x/b = 146 and of the various angles of attack for the case in which the nozzle outlet is at a distance of 40 mm from the plane of the plate. The discharge temperature is T_S = 371° K. In this case we also find universality of the profiles, which again indicates the self-similarity of the flow.

On the basis of these interferograms, we measured the local heat-transfer coefficient at various distances from the nozzle outlet, according to formula (7).

The experimental data for the local values of the Nu(x) number as a function of distance along the plate for various angles of attack φ and various distances l for the nozzle outlet from the plane of the plate are presented in Table 2. These data correspond to a gas flow rate of Q = 1.6 l/sec and a nozzle-outlet tempera-

Table 1

Temperature as a Function of Jet Thickness for Angles of Attack of $\varphi = 30, 60, 90°$

φ=30°	B, mm	0	3	6	9	12	15	18	21	24	27	30
	t, °C	65.0	79.25	77,0	73.5	67.75	61.5	54.0	44.25	34.5	25.5	—
φ=62°	B, mm	0	3	6	9	12	15	18	21	24	27	30
	t, °C	41.0	50.0	47.2	40,0	34.0	29.25	25.0	21.3	—	—	—
φ=90°	B, mm	0	3	6	9	12	15	18	21	24	27	30
	t, °C	22.5	30.5	29.3	26.4	23.5	21.05	—	—	—	—	—

Table 2

Experimental Values for $Nu \cdot 10^{-2}$ at Various Distances from the Nozzle Outlet for Angles of Attack of $\varphi = 0, 30, 60, 90°$

φ°	x, mm				l, mm
	40	80	120	160	
0°	0.80	1.50	2.05	2.65	0
30°	0.92	1.75	2.40	2.72	
60°	1.20	1.98	2.60	2.90	
30°	0.63	1.07	2.30	—	40
60°	0.75	1.80	2.40	—	
90°	0.90	1.90	2.50	2.80	

ture of $T_S = 371°$ K. For angles $\varphi > 0$, the value of x is reckoned from the point at which the axis of the jet intersects the plane of the plate.

At values of $x < 40$, in this experiment the method of determining the heat-transfer coefficient from the interferograms yielded a very great error. It should be noted that the experimental data may be approximated by the following formula [3, 19]:

$$\mathrm{Nu}(x) = 0.1\left[\frac{u_0 x}{\nu}\right]^{0.8}\overline{(x)}^{-k}(\mathrm{Pr})^{0.4}. \qquad (14)$$

The exponent k in [3, 19] is assumed equal to 0.43. However, on the basis of the above-cited experimental data, it follows that k will vary somewhat for various regions of $\overline{x}$. Thus, when $\varphi = 0$, $k = 0.8$ for the regions $\overline{x} = 40-80$, $k = 0.65$ for $\overline{x} = 80-120$, and $k = 0.5$ for $x = 120-180$.

Thus, the inconstancy of k should be taken into consideration in the heat-transfer law (14).

NOTATION

$\delta\lambda$ is the displacement of the interference band; n and n_0 are the refraction indices in disturbed and undisturbed regions, respectively; L is the length of the disturbance region for the refraction index; L_0 is the length of the nozzle slit; x is the distance along the jet distribution with respect to the nozzle outlet; b is the width of the initial jet section; T_S, T_0, and T_m are the temperatures at the nozzle outlet, in the surrounding relatively cold gas and at the jet axis; T_e is the jet temperature near the wall; T_w is the wall temperature; y is the coordinate of the transverse jet section; Nu is the Nusselt number; δ_T is the thickness of the temperature wall boundary layer; b_T is the thickness of the jet boundary layer; B is the total jet thickness; Pr is the Prandtl number; u_0 is the jet velocity at the starting cross section; ν is the kinematic viscosity of the air; a is the structure factor of the plane jet.

REFERENCES

1. O. V. Yakovlevskii and S. Yu. Krashennikov, Mekhanika zhidkosti i gaza [Fluid Dynamics], no. 4, 1966.

2. A. T. Sychev, IFZh, 7, no. 3, 1964.

3. A. L. Kuznetsov and A. V. Sudarev, Energomashinostroenie, no. 6, 1964.

4. M. Jakob, R. Rose, and M. Spielman, Trans. ASME, 72, no. 6, 1950.

5. G. E. Mayers, I. I. Shaver, and R. N. Eustace, Trans. ASME, 85, series C, no. 3, 1963.

6. Ladenburg, Van Voorhis, and Winkler, Voprosy raketnoy tekhniki, nos. 1–2, 60, 43, 1951.

7. G. Kahe and E. Wedemeyer, Phys. Fluids, 72, no. 4, 1964.

8. Collection: Study of Liquid-Propellant Rocket Engines [Russian translation], ed. V. A. Il'inskii, Mir, Moscow, 1964.

9. L. T. Bykov and V. V. Malozemov, IFZh [Journal of Engineering Physics], 8, no. 2, 204, 1965.

10. H. Reihenbach, Wehrtechn. Monatshefte, no. 8, 59, 319, 1962.

11. V. V. Malozemov and I. A. Turchin, IFZh [Journal of Engineering Physics], 8, no. 2, 182, 1965.
12. B. S. Petukhov, A. A. Detlaf, and V. V. Kirillov, ZhTF, vol. XXIV, no. 10, 1954.
13. Z. B. Sakipov, Problems of Thermal Energy and Applied Thermophysics [in Russian], no. 1, Prikladnaya teplofizika, Izv. AN KazSSR, Alma-Ata, 1964.
14. W. Kinder, Optik, 1, 413, 1946.
15. G. N. Abramovich, The Theory of Turbulent Jets [in Russian], Fizmatgiz, 1960.
16. M. F. Romanova, Interference of Light and its Application [in Russian], ONTI, 1937.
17. H. Hannes, Forsch. Geb. Ingenieurswesens, 29, no. 5, 159, 1963.
18. G. N. Abramovich, Turbulent Free Jets of Liquids and Gases [in Russian], Gosenergoizdat, Moscow-Leningrad, 1948.
19. É. P. Volchkov, S. S. Kutateladze, and A. I. Leont'ev, PMTF [Journal of Applied Mechanics and Technical Physics], no. 2, 1965.

7 December 1967

Bauman Higher Technical College, Moscow